FUDMA Journal of Sciences (FJS)
ISSN online: 2616-1370
ISSN print: 2645 - 2944
Vol. 9 No. 9, September, 2025, pp 66 – 77
DOI: https://doi.org/10.33003/fjs-2025-0909-3743

A NOVEL CAPUTO FRACTIONAL-ORDER MODEL OF CHOLERA TRANSMISSION WITH BEHAVIORAL AND IMMUNOLOGICAL DYNAMICS USING THE LAPLACE–ADOMIAN DECOMPOSITION METHOD

Mutairu Kayode Kolawole, Ajimot Folasade Adebisi and *Atinuke Abidemi Adeniji

Department of Mathematical Sciences, Faculty of Basic and Applied Sciences, Osun State University, Osogbo, Nigeria

*Corresponding authors' email: atinukeadeniji0@gmail.com

ABSTRACT

Cholera, spread by the bacterium Vibrio cholerae, is still a major health problem in places with unsanitary conditions. The way it spreads relies on the host's immunity, certain environmental aspects and how clean people keep themselves and their properties. The model in this study applies Caputo fractional-order derivatives to capture the immunity of people, their hygiene, memory in diseases and various ways of controlling them. It includes the study of how people respond and interact with their environment and disease-related factors in a mathematical way. We perform solid analyses on the model, confirming the existence, uniqueness, positivity and boundedness of its solutions. A basic reproduction number is calculated to find out if the disease will continue to exist in a population. Analyzing what makes a disease-free state or an endemic equilibrium stable tells us how to best control the disease. Using the Laplace-Adomian Decomposition Method for solving the nonlinear fractional system results in simulations that match actual cholera behavior. Findings point out that a decline in immunity and better hygiene help reduce how cholera spreads. The framework supports an understanding of cholera spread and is also useful for examining other diseases that are highly complex.

Keywords: Mathematical model, Vibrio cholera, Hygiene, Laplace-Adomian Decomposition Method, Caputo fractional-order, Epidemiological

INTRODUCTION

Cholera has not been fully controlled worldwide, as it is especially dangerous among people who have poor access to sanitation. V. cholerae research is synthesized in this study, especially focusing on how the bacteria become more virulent, how the immune system responds, improvements in vaccines, and the use of models to study the disease (Montero et al., (2023). Even though getting infected provides strong immunity, bestowing immunity for a longer duration is challenging with the existing vaccines (Sit et al., (2022). Modeling has an essential role in understanding how cholera is spread and what tools can help to combat it. Reliable predictions about the beginning of outbreaks are more likely when a fractional-order model with Bayesian neural networks and the Runge–Kutta method is used (Malik, S. (2024). A stochastic model combining neural networks and the Adam optimizer is used to study interventions among different populations (Alharbi, M. F. (2025). A stochastic model that uses the Levenberg–Marquardt algorithm achieves great accuracy when studying infections and environmental changes (Anwar et al., (2025). With the help of stability and sensitivity analyses, SEIRB frameworks confirm the importance of both treatment and early identification (Ali et al., (2025). Modern reviews of studies point out that many of these models are statistical, compartmental, and involve space, advising for the integration of vector-borne cases and accurate estimating of parameters (Anteneh et al., (2024). A Cameroon-based study based on a deterministic SEIRB model reveals spikes in the number of cases happening seasonally and points out the helpfulness of sudden interventions (Nkwayep et al., (2024). Reviews highlight that the disease's spread depends on how and when it appears, human behavior, and how data are organized at different scales (Wang, J. (2022). Also, it explains that aside from the ill, the early spread is mostly due to people with the virus who have no symptoms (Ovi et al., (2025). Simulations from SPRI show that keeping fewer people from the protected group to the susceptible group is a good way to manage support actions. Researchers suggest that acting promptly against an epidemic in Haiti results in a quicker recovery (Avwerosuo et al., (2023); Ratnayake, R. C. (2024); Trevisin et al., (2022). Fractal and fractional models are used now, along with the Caputo-Fabrizio derivative, which offer better performance and indicate important factors contributing to virus spread and limitation (Ahmed et al., (2023); Rashid et al., (2022). They have recently become popular because they model the way diseases with memory act. The Caputo-Fabrizio model pointed out main aspects of vector-borne infections by performing stability and sensitivity analysis (Shah et al., (2025). Models that use fractal-fractional approaches with decay factors demonstrated the behavior of cholera and how people's memories work (Farman et al., (2025); Ahmad et al., (2024). By using decomposition, other fractional methods were able to prove and measure equilibrium behavior and transmission in Ebola and malaria cases (Alhaji et al., (2024).In Sub-Saharan Africa, models for Ebola and malaria also explained the need for quick but long-lasting strategies (Yunus, A. O. & Olayiwola, M. O. (2024). Public health campaigns were proven to work in measles infection models and highlight their importance in controlling the disease (Bashiru et al., (2023); Dhandapani et al., (2023). Studies on cholera disease also highlighted the immediate but limited effect of treatment and the lasting impact vaccination can have (Kolawole, M. K. (2025). Using both types of simulations, experts confirmed that using immunization, treatment, and better sanitation helps in eradicating cholera (Adedeji, J. & Olayiwola, M. O. (2024); Ghosh et al., (2025). There are many new cholera outbreaks happening since 2021, mainly in Africa (Adeniyi, E. O. (2024). Many epidemics have taken place in Nigeria due to weak sanitation, poverty, not enough healthcare support, and changes in the climate. Along with laboratory experiments, there is now a 'stage-switching' model of multidrug-resistant (MDR) cholera, which is supported by both mathematical and numerical analyses (Mushanyu et al., (2024). Various studies make it clear that better WASH infrastructure, more vaccination,

better surveillance, and safe antibiotic use are needed to stop cholera from spreading and causing deaths (Onwunta et al., (2025); Ojo, O. B. & Gbolahan, A. M. (2025); Oweibia et al., (2025); Eneh et al., (2024).

MATERIALS AND METHODS

Model formulation

We first formulate a cholera transmission model using classical integer-order derivatives equation (1) and then reformulate it with the Caputo fractional derivative equation (2) to incorporate memory and hereditary effects. This extension allows for a more realistic representation of behavioral and immunological dynamics in disease spread. The compartmental diagram divides the human population into six epidemiological subgroups, while Table 1 defines the associated variables and parameters. From these formulations, we derive a system of fractional-order differential equations (FODEs), representing a novel Caputo fractional-order cholera model. The system is analyzed and solved

$$\left.\begin{aligned}
\frac{dS}{dt} &= \Lambda - \frac{\beta B(t)S(t)}{K+B(t)} + wR(t) - \mu S(t),\\
\frac{dI}{dt} &= \frac{\beta B(t)S(t)}{K+B(t)} - (\delta + \alpha_1 + \mu)I(t),\\
\frac{dQ}{dt} &= \delta I(t) - (\xi + \alpha_2 + \mu)Q(t),\\
\frac{dR}{dt} &= \xi Q(t) - (w + \mu)R(t),\\
\frac{dB}{dt} &= rB(t) + \eta I(t) - \lambda_1 H(t)B(t) - dB(t),\\
\frac{dH}{dt} &= \rho - \alpha H(t).
\end{aligned}\right\} \quad (1)$$

For simplicity, let the force of infection be constant such that $\lambda = \frac{\beta}{K+B(t)}$

$$\left.\begin{aligned}
CF^Z S(t) &= \Lambda - \lambda B(t)S(t) + wR(t) - \mu S(t),\\
CF^Z I(t) &= \lambda B(t)S(t) - (\delta + \alpha_1 + \mu)I(t),\\
CF^Z Q(t) &= \delta I(t) - (\xi + \alpha_2 + \mu)Q(t),\\
CF^Z R(t) &= \xi Q(t) - (w + \mu)R(t),\\
CF^Z B(t) &= rB(t) + \eta I(t) - \lambda_1 H(t)B(t) - dB(t),\\
CF^Z H(t) &= \rho - \alpha H(t).
\end{aligned}\right\} \quad (2)$$

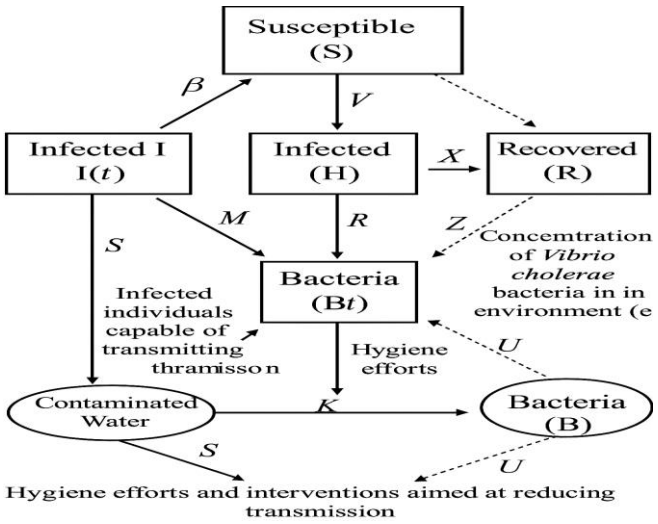

Figure 1: Diagram showing the six (6) subgroups of the total human population

Table 1: Variable and Parameters Definition

Symbols	Definitions
S(t)	Susceptible Population
I(t)	Infected Population
Q(t)	Quarantined Population
R(t)	Recovered Population
B(t)	Bacteria Concentration
H(t)	Hygiene Efforts
K	Half Saturation Constant
$\boldsymbol{\Lambda}$	Recruitment rate
$\boldsymbol{\beta}$	Ingestion rate
W	Immunity waning rate
$\boldsymbol{\mu}$	Natural Death
$\boldsymbol{\delta}$	Quarantine rate
$\boldsymbol{\alpha_1}$	Death rate (Infected)
$\boldsymbol{\varepsilon}$	Recovery rate
$\boldsymbol{\alpha_2}$	Death rate (Quarantine)
R	Natural Growth of Bacteria
$\boldsymbol{\eta}$	Shedding rate
$\boldsymbol{\lambda_1}$	Rate at which Human efforts reduces Bacteria Concentration
D	Bacteria Death rate
$\boldsymbol{\rho}$	Efforts rate to increase hygiene level
$\boldsymbol{\alpha}$	Decay rate of Hygiene effort
$\boldsymbol{\lambda}$	Force of Infection

Positivity and Boundedness of Solution

LEMMA: The Solutions X=(S (t), I (t), Q (t), R(t), Band H (t)) of the fractional order model (4) are non- negative for all $t \geq 0$,with non-negative initial condition inR^6.

Proof: We have the variables at $X^1|_{\varepsilon(V)}$

$$\left.\begin{aligned} &{}^{C}F^{Z}S^{1}(t) = \Lambda + wR(t) \succ 0,\\ &{}^{C}F^{Z}I^{1}(t) = \beta B(t)S(t) \succ 0,\\ &{}^{C}F^{Z}Q^{1}(t) = \delta I(t) \succ 0,\\ &{}^{C}F^{Z}R^{1}(t) = \varepsilon Q(t) \succ 0,\\ &{}^{C}F^{Z}B^{1}(t) = \eta I(t) \succ 0,\\ &{}^{C}F^{Z}H^{1}(t) = \rho \succ 0. \end{aligned}\right\} \quad (3)$$

Where $\varepsilon(v) = [v(t) = 0]$ and $v \in \{S(t), I(t), Q(t), R(t), B(t), H(t)\}$ which exist in$R^6{}_+$. Hence, the model has a bounded positive solution.

LEMMA: Let $\Omega_H$be the domain containing the human population group, $\Omega_B$be the domain of pathogen population and Ω_h be the domain of time- dependent rate of hygiene measure,

Then,

$\Omega_H =$

$$\left[\left(S, I, Q, R \in R^4{}_+ : 0 \leq S + I + Q + R \leq \frac{\Lambda}{\mu}\right]. \quad (4)$$

$$\Omega_B = \left[B \in R: 0 \leq B \leq \frac{\Lambda\alpha\eta}{\mu(\alpha d - \alpha r + \rho\lambda_1)}\right]. \quad (5)$$

and

$$\Omega_h = \left[0 \leq h \leq \frac{\rho}{\alpha}\right]. \quad (6)$$

They are positively invariant.

Proof

From (1) the total human population

$$N = S + I + Q + R: \Lambda - \mu(S + I + Q + R). \quad (7)$$

$$\frac{dN}{dt} = \Lambda - \mu N. \quad (8)$$

$$N(0) = N_0. \quad (9)$$

Solving this linear differential equation at

$$N(t) \leq \frac{\Lambda}{\mu} + \ell^{-\mu t}\left(\eta_0 - \frac{\Lambda}{\mu}\right). \quad (10)$$

$$\text{As } t \to \infty, w(t) \leq \frac{\Lambda}{\mu}. \quad (11)$$

Now

$$\frac{dH}{dt} \leq \rho - \alpha H(t), \text{ solving at } H(0) = h_0. \quad (12)$$

$$H(t) \leq \frac{\rho}{\alpha} + \ell^{-\alpha t}(h_0 - \frac{\rho}{\alpha}) att \to \infty, H(t) = \frac{\rho}{\alpha}. \quad (13)$$

$$\frac{dB}{dt} = rB(t) + \eta I(t) - \lambda_1 H(t)B(t) - dB(t). \quad (14)$$

$$\Longrightarrow \frac{dB}{dt} = rB(t) + \eta(\frac{\Lambda}{\mu}) - \lambda_1(\frac{\rho}{\Lambda}) - dB(t). \quad (15)$$

Solving this linear differential equation at $B(0) = b_0$,

$$B(t) = \frac{\Lambda\alpha\eta}{\mu(\alpha d - \alpha r + \rho\lambda_1)} + \ell^{-\frac{(\alpha d - \alpha r + \rho\lambda_1)}{\alpha}}(b_0 - \frac{\Lambda\alpha\eta}{\mu(\alpha d - \alpha r)}). \text{ as } t = \infty \quad (16)$$

$$B(t) \leq \frac{\Lambda\alpha\eta}{\mu(\alpha d - \alpha r + \rho\lambda_1)}. \quad (17)$$

Thus, three variables are bounded above. Also, since all parameters are positive, $N(t), B(t)$and $H(t)$are all positive. Hence, they belong to a positive invariant region.

Existence and Uniqueness of Solution

In this section, we investigated whether or not the solution to the problem exists and unique. This will help us to know if the model represents a physical problem.

Let,

$$\left.\begin{aligned} M_1 &= \Lambda - \lambda B(t)S(t) + wR(t) - \mu S(t),\\ M_2 &= \lambda B(t)S(t) - (\delta + \alpha_1 + \mu)I(t),\\ M_3 &= \delta I(t) - (\xi + \alpha_2 + \mu)Q(t),\\ M_4 &= \xi Q(t) - (w + \mu)R(t),\\ M_5 &= rB(t) + \eta I(t) - \lambda_1 H(t)B(t) - dB(t),\\ M_6 &= \rho - \alpha H(t), \end{aligned}\right\} \quad (18)$$

Then,

$\left|\frac{\partial M_1}{\partial S}\right| = -\lambda B - \mu; \left|\frac{\partial M_1}{\partial I}\right| = 0; \quad \left|\frac{\partial M_1}{\partial Q}\right| = 0; \left|\frac{\partial M_1}{\partial R}\right| = w; \left|\frac{\partial M_1}{\partial B}\right| = 0; \left|\frac{\partial M_1}{\partial H}\right| = 0.$

$\left|\frac{\partial M_2}{\partial S}\right| = \lambda B; \left|\frac{\partial M_2}{\partial I}\right| = -(\delta + \alpha_1 + \mu); \left|\frac{\partial M_2}{\partial Q}\right| = 0; \left|\frac{\partial M_2}{\partial R}\right| = 0; \left|\frac{\partial M_2}{\partial B}\right| = 0; \left|\frac{\partial M_2}{\partial H}\right| = 0.$

$\left|\frac{\partial M_3}{\partial S}\right| = 0; \left|\frac{\partial M_3}{\partial I}\right| = \delta; \left|\frac{\partial M_3}{\partial Q}\right| = -(\xi + \alpha_2 + \mu); \quad \left|\frac{\partial M_3}{\partial R}\right| = 0; \left|\frac{\partial M_3}{\partial B}\right| = 0; \left|\frac{\partial M_3}{\partial H}\right| = 0.$

$\left|\frac{\partial M_4}{\partial S}\right| = 0; \left|\frac{\partial M_4}{\partial I}\right| = 0; \left|\frac{\partial M_4}{\partial Q}\right| = \xi; \quad \left|\frac{\partial M_4}{\partial R}\right| = -(w + \mu); \left|\frac{\partial M_4}{\partial B}\right| = 0; \left|\frac{\partial M_4}{\partial H}\right| = 0.$

$\left|\frac{\partial M_5}{\partial S}\right| = 0; \left|\frac{\partial M_5}{\partial I}\right| = \eta; \left|\frac{\partial M_5}{\partial Q}\right| = 0 \ ;$

$\left|\frac{\partial M_5}{\partial R}\right| = 0; \left|\frac{\partial M_5}{\partial B}\right| = r - \lambda_1 H - d; \left|\frac{\partial M_5}{\partial H}\right| = -\lambda_1 B.$

$\left|\frac{\partial M_6}{\partial S}\right| = 0; \left|\frac{\partial M_6}{\partial I}\right| = 0; \left|\frac{\partial M_6}{\partial Q}\right| = 0 \quad ; \quad \left|\frac{\partial M_6}{\partial R}\right| = 0; \left|\frac{\partial M_6}{\partial B}\right| = 0; \left|\frac{\partial M_6}{\partial H}\right| = -\alpha.$

Hence, since the partial derivative exists, the solution to the problem is continuous and bounded, therefore the model represents a physical problem and it is well posed.

Disease Free Equilibrium

This is a state where a disease is no longer present or prevalent in a population. For the disease-free equilibrium, I=0, B=0, Thus, solving at steady states

Let CF^ZS = CF^ZI = CF^ZQ = CF^ZR = CF^ZB = CF^ZH= 0.

$\overset{0}{S} = \overset{0}{I} = \overset{0}{Q} = \overset{0}{R} = \overset{0}{B} = \overset{0}{H} = 0$,DFE is given by;

$S = \frac{\Lambda}{\mu}, I = 0, Q = 0, R = 0, B = 0, H = \frac{\rho}{\alpha}.$

$$E_0 = \left(\frac{\Lambda}{\mu}, 0,0,0,0, and \frac{\rho}{\alpha}\right). \quad (19)$$

Endemic Equilibriums

This is a state where a disease is consistently present and prevalent in a population, but at a relatively stable and low level.

At this steady state, $B \neq I \neq O$.

Thus, solving, we obtained

$$S^* = \frac{(\delta+\mu+\alpha_1)(\alpha d - \alpha r - \lambda\rho)}{\alpha\eta k}. \quad (20)$$

$$Q^* = \frac{\delta(\alpha d - \alpha r - \lambda\rho)}{\alpha\eta}. \quad (21)$$

$$I^* = \frac{[(\Lambda k\eta - (\delta+\mu+\alpha_1)\mu(d-r)(w+\mu) + \delta w\varepsilon k(d-r)]\alpha - [-\delta\varepsilon kw + \lambda\rho[(\delta+\mu+\alpha_1)(w+\mu)\mu]}{(\delta+\mu+\alpha_1)(w+\mu)k\alpha\eta}. \quad (22)$$

$$R^* = \frac{\varepsilon\delta(\alpha d - \alpha r - \lambda\rho)}{\alpha\eta}. \quad (23)$$

$$B^* = \frac{I^*\alpha\eta}{(\alpha d - \alpha r - \lambda\rho)}. \quad (24)$$

$$H^* = \frac{\rho}{\alpha}. \quad (25)$$

Basic Reproduction Number (R_0)

According to Anderson (2018), the basic reproduction number $R_0$is defined as the average number of secondary cases generated by a single infective individual in a completely susceptible population. This is calculated using the next-generation matrix method as follows;

$R_0 = \sigma(FV^{-1})$ such that $\sigma$is the spectral radius,

$$F = \begin{bmatrix} f_1 \\ f_2 \\ f_3 \\ f_4 \\ f_5 \\ f_6 \end{bmatrix} = \begin{bmatrix} 0 \\ \lambda SB \\ 0 \\ 0 \\ 0 \\ 0 \end{bmatrix}. \quad (26)$$

$$V=\begin{bmatrix}v_1\\v_2\\v_3\\v_4\\v_5\\v_6\end{bmatrix}=\begin{bmatrix}\Lambda+wR-\lambda\beta S-\mu S\\-(\delta+\mu+\alpha_1)I\\\delta I-(\varepsilon+\alpha_2+\mu)Q\\\varepsilon Q-(w+\mu)R\\rB+\eta I-\lambda_1 HB-dB\\\rho-\alpha H\end{bmatrix}. \quad (27)$$

$$F\times V^{-1}=\begin{bmatrix}0&0&0&0&0&0\\0&\frac{\lambda\eta\Lambda\alpha}{\mu(\delta+\mu+\alpha_1)(\alpha d-\alpha r+\lambda\rho)}&0&0&\frac{\lambda\Lambda\alpha}{\mu(\alpha d-\alpha r+\lambda\rho)}&0\\0&0&0&0&0&0\\0&0&0&0&0&0\\0&0&0&0&0&0\\0&0&0&0&0&-\alpha\end{bmatrix}. \quad (28)$$

Hence, $R_0=\frac{\lambda\eta\Lambda\alpha}{\mu(\delta+\mu+\alpha_1)(\alpha d-\alpha r+\lambda\rho)}$. (29)

Equation (29) gives Basic Reproduction Number (R_0)

Local Stability of Disease-Free Equilibriums

To examine the Local Stability of DFE point, we obtain the Jacobian matrix of (4) such that

$$J=\begin{bmatrix}-(Bk+\mu)&0&0&w&-kS&0\\Bk&-(\delta+\mu+\alpha_1)&0&0&kS&0\\0&\delta&-(\varepsilon+\alpha_2+\mu)&0&0&0\\0&0&\varepsilon&-(\mu+w)&0&0\\0&\eta&0&0&-(H\lambda+d+r)&0\\0&0&0&0&0&-\alpha\end{bmatrix}. \quad (30)$$

$\lambda_1=-\alpha_1.$

$\lambda_2=-\mu.$

$\lambda_3=-D.$

$\lambda_4=-C.$

$\lambda_5=\frac{-1}{2}[B+E+\delta\sqrt{(B-E)^2+4A\eta}].$

$\lambda_6=\frac{-1}{2}[B+E+\sqrt{(B-E)^2+4A\eta}].$

Local Stability of Endemic Equilibrium Point

Theorem: - The regional resilience of the persistence equilibrium of the proposed model is locally asymptotically stable if $R_0<1$ and unstable if otherwise.

Proof: - Suppose,$S=a+S^*, I=b+I^*, Q=c+Q^*, R=x+R^*, B=y+B^*, H=f+H^*.$

Linearizing equation (1) to obtain $\frac{da}{dt}=\Lambda-\lambda ay+wx-\mu a.$

The characteristic equation obtained from its Jacobian matrix is as follows;

$$J=\begin{bmatrix}-(B\lambda+\mu)&0&0&w&-\lambda S&0\\B\lambda&-(\delta+\mu+\alpha_1)&0&0&\lambda S&0\\0&\delta&-(\varepsilon+\alpha_2+\mu)&0&0&0\\0&0&\varepsilon&-(\mu+w)&0&0\\0&\eta&0&0&-(H\lambda+d+r)&-\lambda B\\0&0&0&0&0&-\alpha\end{bmatrix}. \quad (31)$$

The resulting eigen value of the above matrix is obtained as

$\lambda^6-[(p+q+s)(r+w+w)+pq+rs]+\lambda^5[(p+t)(q+s)+tw+rs]-[pqs(r+q)+pt(r+t)\lambda^4[qtw(p+q)+qr(p+q+s)]\lambda^3+[pt+ps+qs+pr]\lambda^2+[(t+p)(q+r)]\lambda^1+pqrstw=0.$

Therefore, the regional resilience of the Eigen values in the model invariant region of ${R_6}^+$ is asymptotically stable.

Global Stability of the Disease Free Equilibrium

To analyses the global stability of the disease-free equilibrium (DFE) of the given cholera model, at DFE, the infected compartments (I, Q, B) =0 i.e. the disease is absent in the population.

Setting I=0, Q=0, B=0 in the system, we solve for the equilibrium values of the remaining variables;

$E_0=(S^*,I^*,Q^*,R^*,B^*,H^*).$

$E_0=(\frac{\Lambda}{\mu},0,0,0,0,\frac{\rho}{\alpha}\ ).$ (32)

$\frac{dV}{dt}=a_1(\lambda B\frac{\Lambda}{\mu}-(\delta+\alpha_1+\mu)I+a_2\delta I-(\xi+\alpha_2+\mu)Q+a_3rB+\eta Q-\lambda_1 H^*B-dB,)$

$\frac{dV}{dt}=a_1\lambda B\frac{\Lambda}{\mu}-a_1(\delta+\alpha_1+\mu)I+a_2\delta I-a_2(\xi+\alpha_2+\mu)Q+a_3rB+a_3\eta Q-a_3\lambda_1 H^*B-a_3dB,$ (33)

$\frac{dV}{dt}=(a_1\lambda\frac{\Lambda}{\mu}+a_3r-a_3\lambda_1H^*-a_3\lambda_1H^*)B+(-a_1(\delta+\alpha_1+\mu)+a_2\delta)I+(-a_2(\xi+a_2+\mu)+a_3\eta)Q,$

Choosing a_1,a_2,a_3 such that

$a_1(\delta+\alpha_1+\mu)>a_2\delta,\ a_1\lambda\frac{\Lambda}{\mu}+a_3r<a_3\lambda_1H^*-a_3d,$then $\frac{dV}{dt}\le 0$ (34)

Since all terms are non-positive and zero only at the DFE, this proves global asymptotically stable'

Therefore, if$R_0 < 1$, then $\frac{dV}{dt} \leq 0$and E_0 is globally asymptotically stable (i.e. Cholera dies out over time, regardless of initial conditions).

Global Stability of Endemic Equilibrium

THEOREM: - If $S = S^*, I = I^*, Q = Q^*, R = R^*, B = B^* and H = H^*andY \prec W$, with unstable $R < 1$,then system (4) is globally asymptotically stable for$R_0 > 1$.

PROOF: - The Lyaponuv function is used to obtain global stability utilizing the developed Lyaponuv function by Cai and Li (2012).

$$P = (S^*, I^*, Q^*, R^*, B^*, H^*) = (S - S^* - S^* log \frac{S}{S^*}) + (I - I^* - I^* log \frac{I}{I^*}) + (Q - Q^* - Q^* log \frac{Q}{Q^*}) + (R - R^* - R^* log \frac{R}{R^*}) + (B - B^* - B^* log \frac{B}{B^*}) + (H - H^* - H^* log \frac{H}{H^*}) \quad (35)$$

Through direct calculation, we derive the Lyaponuv function for the solution of equation (43) as follows;

$$\frac{dP}{dt} = \frac{dS}{dt} - \left(\frac{S}{S^*}\right)\frac{dS}{dt} + \frac{dI}{dt} - \left(\frac{I}{I^*}\right)\frac{dI}{dt} + \frac{dQ}{dt} - \left(\frac{Q}{Q^*}\right)\frac{dQ}{dt} + \frac{dR}{dt} - \left(\frac{R}{R^*}\right)\frac{dR}{dt} + \frac{dB}{dt} - \left(\frac{B}{B^*}\right)\frac{dB}{dt} + \frac{dH}{dt} - \left(\frac{H}{H^*}\right)\frac{dH}{dt} \quad (36)$$

$$\frac{dP}{dt} = \Lambda - \lambda B(t)S(t) + wR(t) - \mu S(t) - \left(\frac{S}{S^*}\right)\Lambda - \lambda B(t)S(t) + wR(t) - \mu S(t) + \lambda B(t)S(t) - (\delta + \alpha_1 + \mu)I(t) - \left(\frac{I}{I^*}\right)\lambda B(t)S(t) - (\delta + \alpha_1 + \mu)I(t) + \delta I(t) - (\xi + \alpha_2 + \mu)Q(t) - \left(\frac{Q}{Q^*}\right)\delta I(t) - (\xi + \alpha_2 + \mu)Q(t) + \xi Q(t) - (w + \mu)R(t) - \left(\frac{R}{R^*}\right)\xi Q(t) - (w + \mu)R(t) + rB(t) + \eta I(t) - \lambda_1 H(t)B(t) - dB(t) - \left(\frac{B}{B^*}\right)rB(t) + \eta I(t) - \lambda_1 H(t)B(t) - dB(t) + \rho - \alpha H(t) - \left(\frac{H}{H^*}\right)\rho - \alpha H(t) \quad (37)$$

Since the polynomial has a positive sign throughout analysis, Descartes's rule of signs is satisfied. Therefore, the polynomial cannot have any negative roots that are real numbers. After this result, applying the Routh Hurwitz condition gives another way to look at the polynomial and highlights its unique features.

$$\frac{dP}{dt} = \Lambda - \lambda B(t)S(t) + wR(t) - \mu S(t) - \left(\frac{S}{S^*}\right)\Lambda + \left(\frac{S}{S^*}\right)[\lambda B(t)S(t) - wR(t) + \mu S(t)] + \lambda B(t)S(t) - (\delta + \alpha_1 + \mu)I(t) - \left(\frac{I}{I^*}\right)\lambda B(t)S(t) + \left(\frac{I}{I^*}\right)(\delta + \alpha_1 + \mu)I(t) + \delta I(t) - (\xi + \alpha_2 + \mu)Q(t) - \left(\frac{Q}{Q^*}\right)\delta I(t) + \left(\frac{Q}{Q^*}\right)(\xi + \alpha_2 + \mu)Q(t) + \xi Q(t) - (w + \mu)R(t) - \left(\frac{R}{R^*}\right)\xi Q(t) + \left(\frac{R}{R^*}\right)(w + \mu)R(t) + rB(t) + \eta I(t) - \lambda_1 H(t)B(t) - dB(t) - \left(\frac{B}{B^*}\right)rB(t) + \eta I(t) + \left(\frac{B}{B^*}\right)[\lambda_1 H(t)B(t) - dB(t) + \rho - \alpha H(t) - \left(\frac{H}{H^*}\right)\rho\left(\frac{H}{H^*}\right)\alpha H(t) \quad (38)$$

By rearranging terms i.e both positive and negative terms we have,

$$\frac{dP}{dt} = Y - W\ Y = \Lambda - \lambda B(t)S(t) + wR(t) - \mu S(t) + \left(\frac{S}{S^*}\right)[\lambda B(t)S(t) - wR(t) + \mu S(t)] + \lambda B(t)S(t) - (\delta + \alpha_1 + \mu)I(t) + \left(\frac{I}{I^*}\right)(\delta + \alpha_1 + \mu)I(t) + \delta I(t) - (\xi + \alpha_2 + \mu)Q(t) + \left(\frac{Q}{Q^*}\right)(\xi + \alpha_2 + \mu)Q(t) + \xi Q(t) - (w + \mu)R(t) + \left(\frac{R}{R^*}\right)(w + \mu)R(t) + rB(t) + \eta I(t) - \lambda_1 H(t)B(t) - dB(t) + \left(\frac{B}{B^*}\right)[\lambda_1 H(t)B(t) - dB(t) + \rho - \alpha H(t) + \left(\frac{H}{H^*}\right)\alpha H(t) \quad (39)$$

And

$$W = -\left(\frac{S}{S^*}\right)\Lambda - \left(\frac{I}{I^*}\right)\lambda B(t)S(t) - \left(\frac{Q}{Q^*}\right)\delta I(t) - \left(\frac{R}{R^*}\right)\xi Q(t) - \left(\frac{B}{B^*}\right)rB(t) + \eta I(t) - \left(\frac{H}{H^*}\right)\rho \quad (40)$$

Hence, if $Y < W$, then $\frac{dP}{dt}$=0 if and only if

$$S = S^*, I = I^*, Q = Q^*, R = R^*, B = B^* \text{and} H = H^* \quad (41)$$

Thus, we have the largest compartment invariant set to be equal to $\left\{(S^*, I^*, Q^*, R^*, B^*, H^*) \in \Gamma, \frac{dP}{dt} = 0\right\}$ where $E^*$is a singleton of the endemic equilibrium. For this reason, the Lasalle's invariant approach shows that Γif$Y < W$, the$E^*$is globally asymptotically stable.

Numerical Simulation

Application of Laplace-Adomian Decomposition Method (LADM)

Using LADM, the equation is solved and the solution, an analytical series, is found by decomposing difficult non-linear functions into easy-to-calculate Adomian polynomials. Hence, LADM uses the formula below to solve equation (4).

With initial conditions;

$$S(0) = S_0, I(0) = I_0, Q(0) = Q_0, R(0) = R_0, B(0) = B_0. H(0) = H_0$$

$$\begin{aligned} &L\{CF^z S(t)\} = L\{\Lambda - \lambda B(t)S(t) + wR(t) - \mu S(t)\}, \\ &L\{cF^z I(t)\} = L\{\lambda B(t)S(t) - (\delta + \alpha_1 + \mu)I(t)\}, \\ &L\{cF^z Q(t)\} = L\{\delta I(t) - (\xi + \alpha_2 + \mu)Q(t)\}, \\ &L\{cF^z R(t)\} = L\{\xi Q(t) - (w + \mu)R(t)\}, \\ &L\{cF^z B(t)\} = L\{rB(t) + \eta I(t) - \lambda_1 H(t)B(t) - dB(t)\}, \\ &L\{cF^z H(t)\} = L\{\rho - \alpha H(t)\}. \end{aligned} \quad (42)$$

Let S, I, Q, R, B and H be infinite series such that;

$$S = \sum_{i=0}^{z} S_i, I = \sum_{i=0}^{z} I_i, Q = \sum_{i=0}^{z} Q_i, R = \sum_{i=0}^{z} R_i, B = \sum_{i=0}^{z} B_i, H = \sum_{i=0}^{z} H_i \quad (43)$$

BS and HB are non- linear term of the model and it can be broken down by Adomian. Let

$$BS = \sum_{i=0}^{z} M_i \text{and } HB = \sum_{i=0}^{z} N_i \quad (44)$$

Where $M_i$and $N_i$are Adomian polynomial such that:

$$M_i = \frac{1}{\Gamma(i+1)}\frac{d^i}{d\lambda^i}[\sum_{x=0}^{\infty}\lambda^x B_x \sum_{x=0}^{\infty}\lambda^x S_x]_{\lambda=0} \text{and} \quad (45)$$

$$N_i = \frac{1}{\Gamma(i+1)}\frac{d^i}{d\lambda^i}[\sum_{x=0}^{\infty}\lambda^x H_x \sum_{x=0}^{\infty}\lambda^x B_x]_{\lambda=0} \quad (46)$$

Taking

$$S_0 = v_1, I_0 = v_2, Q_0 = v_3, R_0 = v_4, B_0 = v_5, H_0 = v_6, \quad (47)$$

$$S_1(t) = t^z(\Lambda - v_1(\lambda v_5 + \mu) + v_4 w)\frac{1}{\Gamma(1+z)} \quad (48)$$

$$I_1(t) = t^z(\lambda v_1 v_5 - (\delta + \alpha_1 + \mu)v_2\frac{1}{\Gamma(1+z)}) \quad (49)$$

$$Q_1(t) = t^z(v_2\delta - v_3(\varepsilon + \alpha_2 + \mu)\frac{1}{\Gamma(1+z)}) \quad (50)$$

$$R_1(t) = t^z(v_3\varepsilon - v_4(w+\mu)\frac{1}{\Gamma(1+z)} \quad (51)$$

$$B_1(t) = t^z(v_5(r - \lambda_1 v_6 - d) + \eta v_2)\frac{1}{\Gamma(1+z)} \quad (52)$$

$$H_1(t) = t^z(\rho - \alpha v_6)\frac{1}{\Gamma(1+z)} \quad (53)$$

$$S_2(t) = \left\{\Lambda - \lambda(v_5[(\Lambda - v_1(\lambda v_5 + \mu) + w v_4\}\frac{t^{2z}}{\Gamma(1+2z)} + v_1[v_5(r - \lambda_1 v_6 - d) + \eta v_2\right\}\frac{t^{2z}}{\Gamma(1+2z)} + w\left[v_3\varepsilon - v_4(w + \mu)\right]\frac{t^{2z}}{\Gamma(1+2z)} - \mu\left[\Lambda - v_1(\lambda v_5 + \mu) + v_4 w\right)\frac{t^{2z}}{\Gamma(1+2z)}\right] \quad (54)$$

$$I_2(t) = \lambda v_5\left[(\Lambda - v_1(\lambda v_5 + \mu) + v_4 w]\frac{t^{2z}}{\Gamma(1+2z)} + v_1[v_5(r - \lambda_1 v_6 - d) + \eta v_2]\frac{t^{2z}}{\Gamma(1+2z)} - (\delta + \alpha_1 + \mu)\{\lambda v_1 v_5 - (\delta + \alpha_1 + \mu)v_2\frac{t^{2z}}{\Gamma(1+2z)}\right. \quad (55)$$

$$Q_2(t) = \delta(\lambda v_1 v_5 - (\delta + \alpha_1 + \mu)v_2]\frac{t^{2z}}{\Gamma(1+2z)} - (\varepsilon + \alpha_2 + \mu)[v_2\delta - v_3(\varepsilon + \alpha_2 + \mu))\frac{t^{2z}}{\Gamma(1+2z)} \quad (56)$$

$$R_2(t) = \varepsilon\{v_2\delta - v_3(\varepsilon + \alpha_2 + \mu)\frac{t^{2z}}{\Gamma(1+2z)} - (w+\mu)[v_3\varepsilon - v_4(w+\mu)\frac{t^{2z}}{\Gamma(1+2z)} \quad (57)$$

$$B_2(t) = r\{t^z[v_5(r - \lambda_1 v_6 - d) + \eta v_2)\frac{t^{2z}}{\Gamma(1+2z)} + \eta t^z\{\lambda v_1 v_5 - (\delta + \alpha_1 + \mu)v_2\frac{t^{2z}}{\Gamma(1+2z)} - \lambda_1\{v_6 t^z[v_5(r - \lambda_1 v_6 - d) + \eta v_2]\frac{t^{2z}}{\Gamma(1+2z)} + t^z v_5(\rho - \alpha v_6)\frac{t^{2z}}{\Gamma(1+2z)}] - dt^z[v_5(r - \lambda_1 v_6 - d) + \eta v_2]\frac{t^{2z}}{\Gamma(1+2z)} \quad (58)$$

$$H_2(t) = (\rho - \alpha)(\rho - \alpha v_6)\frac{t^{2z}}{\Gamma(1+2z)} \quad (59)$$

$$t^z(\Lambda - v_1(\lambda v_5 + \mu) + v_4 w)\frac{1}{\Gamma(1+z)}$$

Table 2: Parameter Values and Initial Conditions for the SIQRB Model

Parameter	Description	Value	Reference
Λ	Recruitment rate	$24.4N(0)/365000\ (\text{day}^{-1})$	Trevisin et al., (2022)
μ	Natural death rate	$2.2493 \times 10^{-5}\ (\text{day}^{-1})$	Trevisin et al., (2022)
λ	Force of infection	$0.8\ (\text{day}^{-1})$	Trevisin et al., (2022)
r	Multiplication rate of bacteria via binary fission	$4.158(\text{day}^{-1})$	Assumed
ω	Immunity waning rate	$0.4/365\ (\text{day}^{-1})$	Trevisin et al., (2022)
δ	Quarantine rate	$0.05\ (\text{day}^{-1})$	Assumed
$l\grave{o}$	Recovery rate	$0.2\ (\text{day}^{-1})$	Trevisin et al., (2022)
α_1	Death rate (infected)	$0.015\ (\text{day}^{-1})$	Trevisin et al., (2022)
α_2/'	Death rate (quarantined)	$0.0001\ (\text{day}^{-1})$	Trevisin et al., (2022)
η	Shedding rate (infected)	$10\ (\text{cell/mlday}^{-1}\text{person}^{-1})$	Trevisin et al., (2022)
λ_1	Clearance rate of pathogens due to hygienic measure	$0.3, 0 \leq \lambda_1 \leq 1,$	Assumed
ρ	Investment (Effort) rate to increase hygiene levels.	0.5	Assumed
A	the natural decay of hygiene measures (e.g., infrastructure decay or reduced public	$0.3, 0 \leq \lambda_1 \leq 1,$	Assumed
d	Bacteria death rate	$0.33\ (\text{day}^{-1})$	Trevisin et al., (2022)
$S(0)$	Susceptible individuals at $t = 0$	$570\ (\text{person})$	Assumed
$I(0)$	Infected individuals at $t = 0$	$170\ (\text{person})$	
$Q(0)$	Quarantined individuals at $t = 0$	$0\ (\text{person})$	Assumed
$R(0)$	Recovered individuals at $t = 0$	$0\ (\text{person})$	Assumed
$B(0)$	Bacterial concentration at $t = 0$	$275 \times 10^3\ (\text{cell/ml})$	Assumed

Table 2 above summarizes the parameter values and initial conditions used in the SIQRB model. These include key rates such as transmission, recovery, quarantine, and bacterial growth, along with the initial population values for S(0), I(0), Q(0), R(0), and B(0). The table provides the baseline setup necessary for simulating the cholera transmission dynamics.

RESULTS AND DISCUSSION

Simulation Result

Utilizing the results obtained from LADM with Caputo derivatives on equation (9) and parameter values in Table 1, we perform numerical simulations to observe how the system acts in various situations. They study in detail how immunity problems following treatment and interventions to raise hygiene affect the way diseases are passed on. The study

looks at how these factors cause changes in the number of susceptible, infected and pathogen individuals so that its role in the disease spread can be better understood. The analysis gives understanding of the link between hygiene control and the number of people experiencing relapses, indicating possible steps to reduce infections and improve handling of diseases.

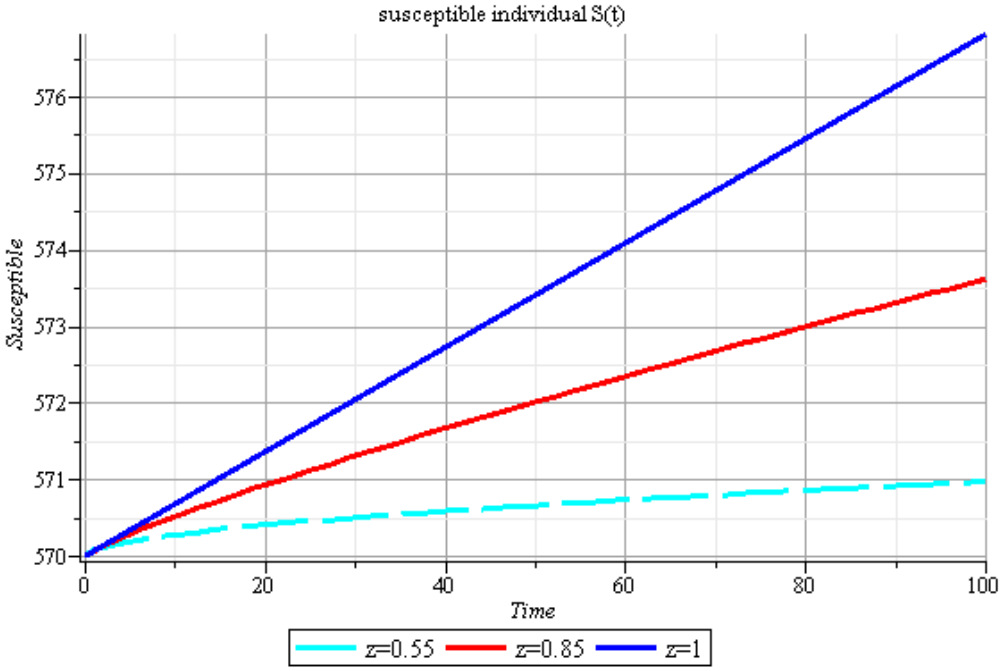

Figure 2: Plot shows the behavior of S(t) at different values of fractional order z

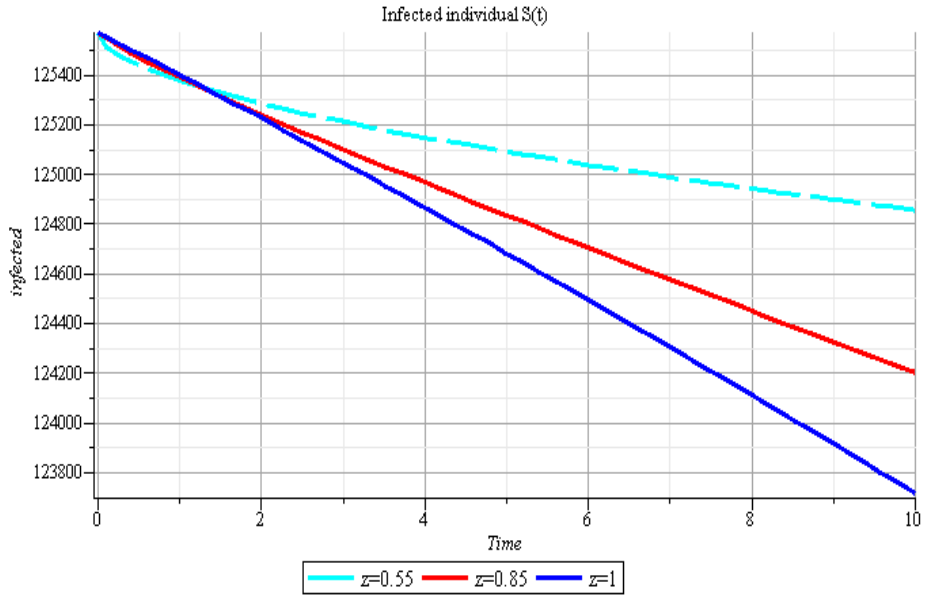

Figure 3: Plot shows the behavior of I(t) at different values of fractional order z

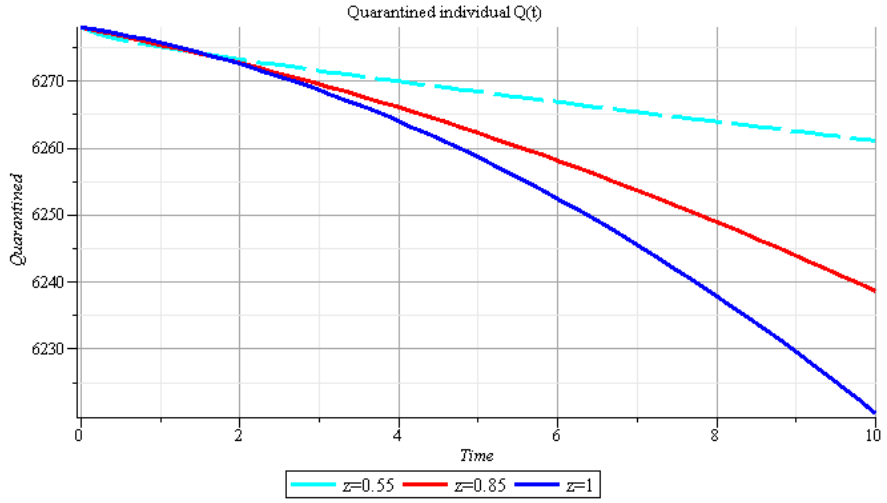

Figure 4: Plot shows the behavior of Q(t) at different values of fractional order z

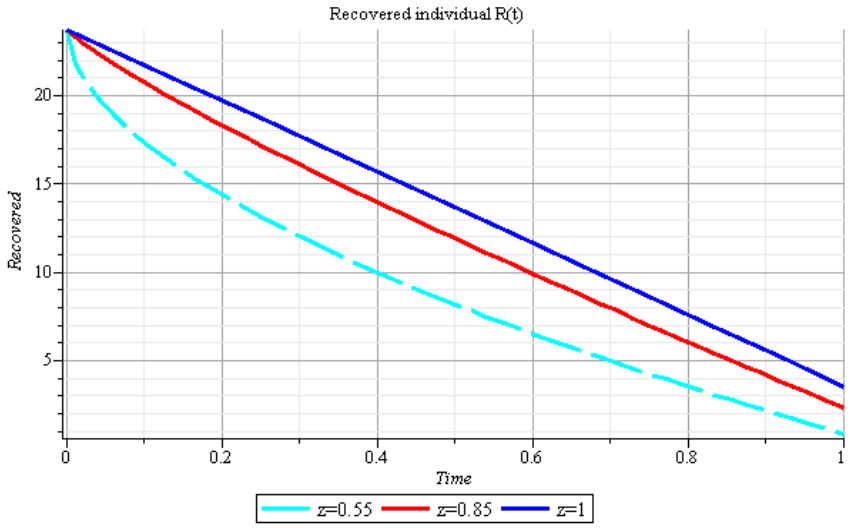

Figure 5: Plot shows the behavior of R(t) at different values of fractional order z

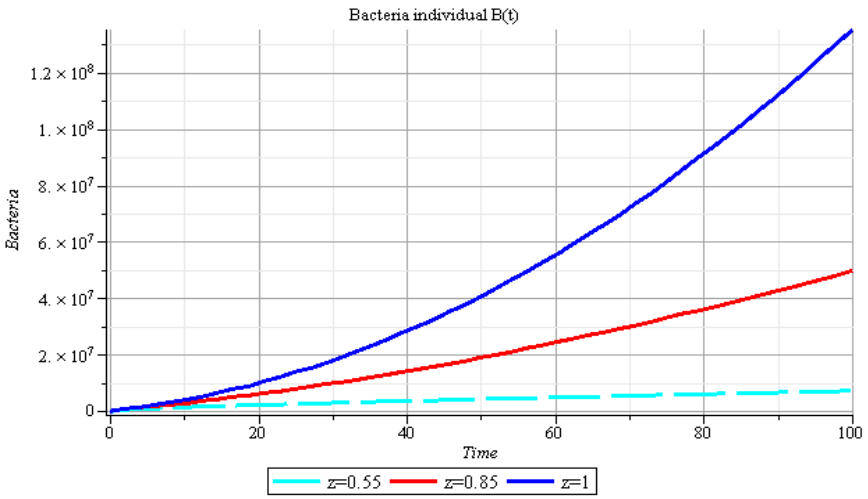

Figure 6: Plot shows the behavior of B(t) at different values of fractional order z

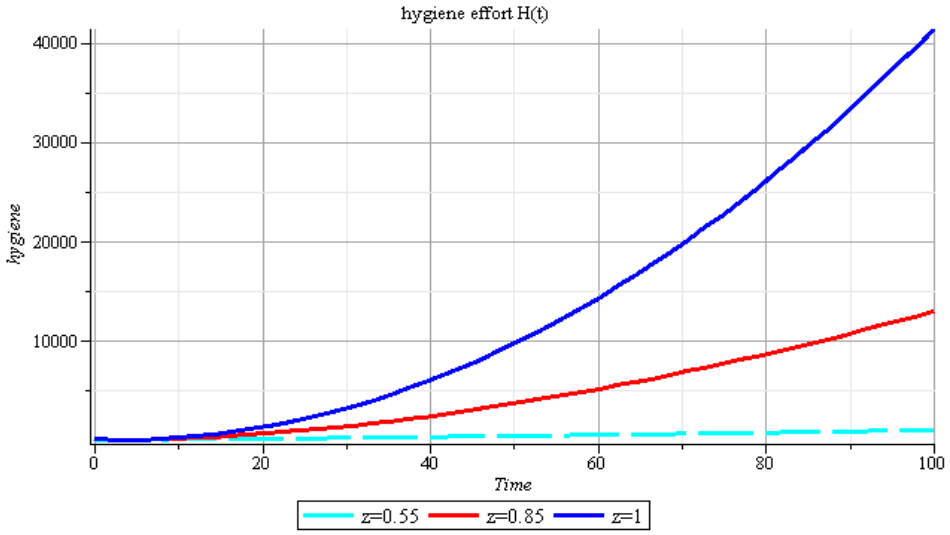

Figure 7: Plot shows the behavior of H(t) at different values of fractional order z

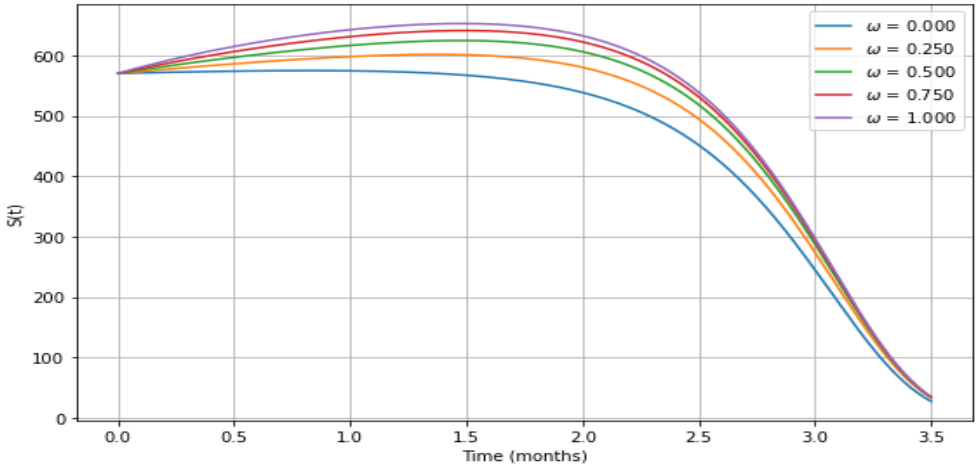

Figure 8: Effect of Relapse rate of recovered individuals post immunity gained from treatment on S(t)

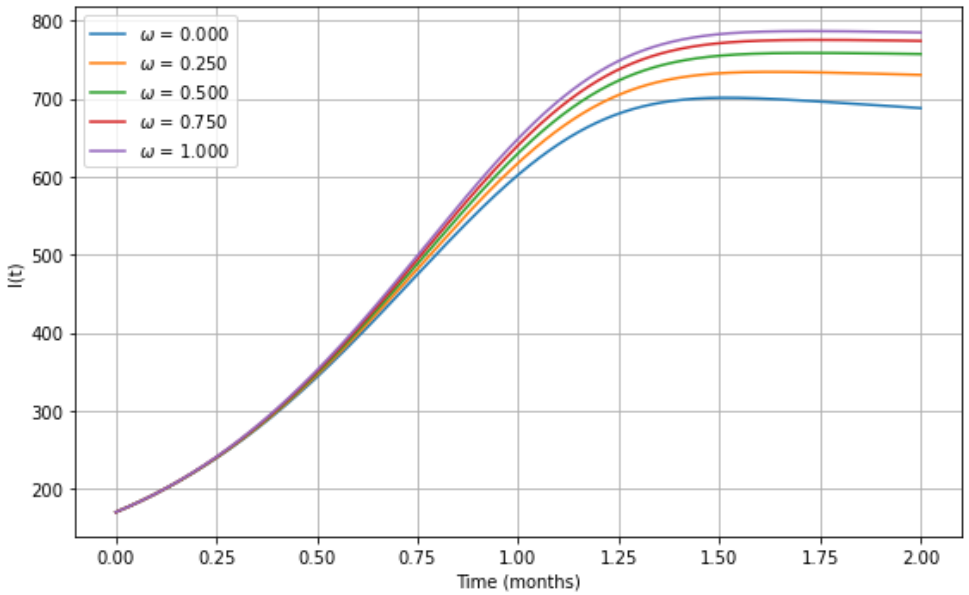

Figure 9: Effect of Relapse rate of recovered individuals post immunity gained from treatment on I(t)

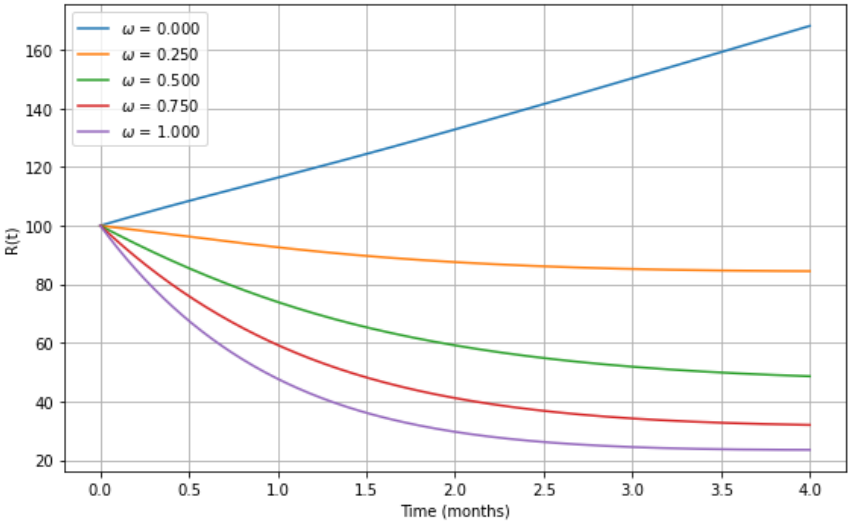

Figure 10: Effect of Relapse rate of recovered individuals post immunity gained from treatment on I(t)

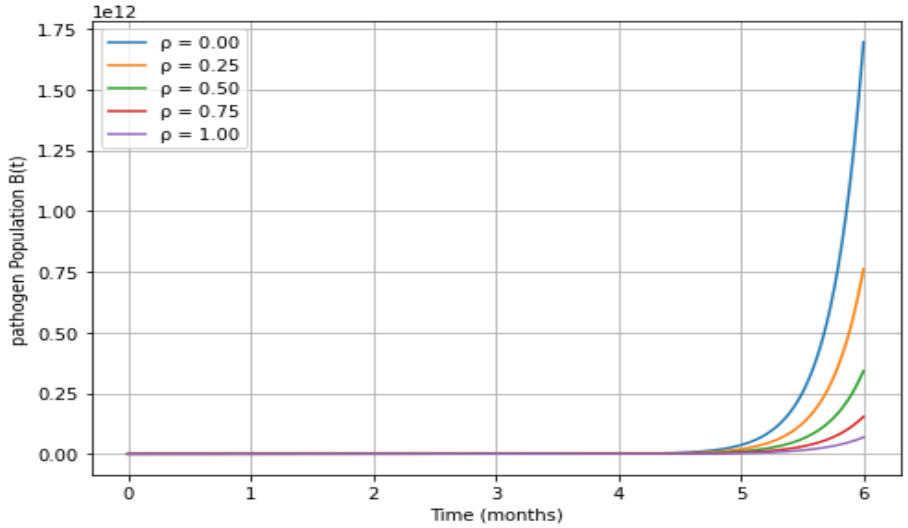

Figure 11: Effect of effort rate to increase hygienic level on pathogen population

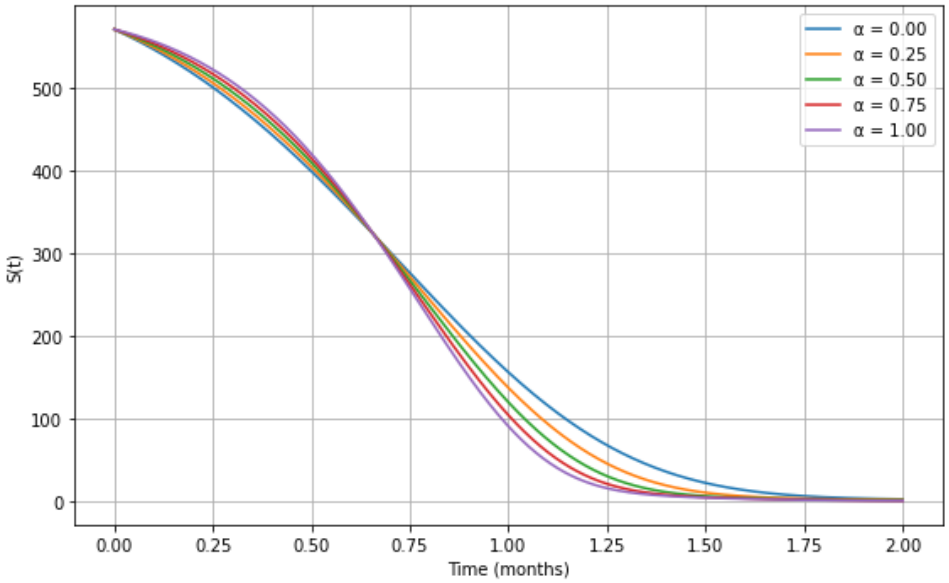

Figure 12: Impact of decay rate of hygienic efforts on Susceptible population

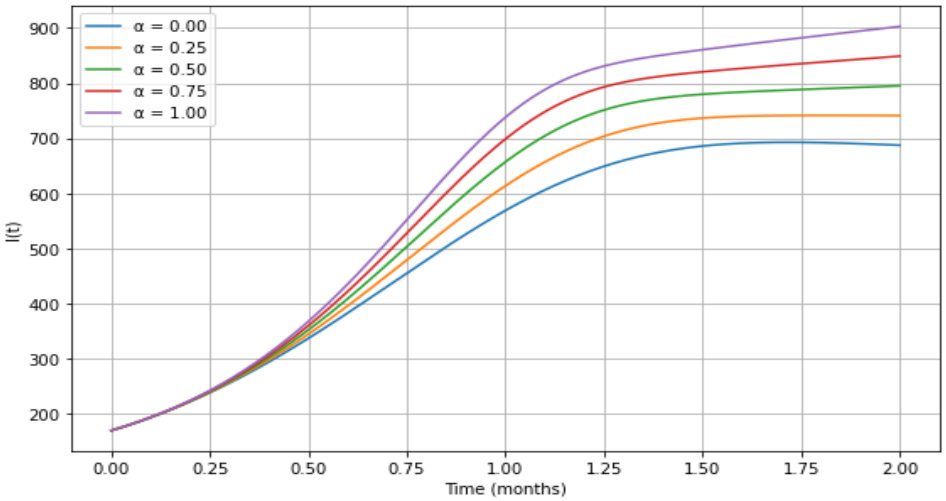

Figure 13: Impact of decay rate of hygienic efforts on Infected population

Discussion

The use of simulations allows a clear view of the impact of fractional-order behaviors and interventions on the disease's transmission. As shown in Figure 1, more extensive disease exposure is predicted when the fractional orders are higher, because the susceptible population decreases more slowly. A lower z in Figure 2 means there is less of an increase in the infected population, showing that stronger memory effects lead to the disease slowing down in progression. Figure 3 demonstrates that the size of the quarantined population depends highly on how far z is from 1 which stresses the importance of memory when making intervention decisions. Also, delayed healing is demonstrated in Figure 4 with z showing greater influence on protecting against another infection. The mental health of a person can lead to changes in their environment and behaviors. Evident from Figure 5, the environment can be kept cleaner as z increases, meaning that the chances of bacterial overgrowth go down, while Figure 6 displays that improving behavioral memory allows people to keep up good hygiene habits over time. Figures 7 to 9 examine the growth in relapse rates which results in increases in the numbers of susceptible individuals (Figure 7) and infected people (Figures 8 and 9), highlighting the importance of lasting immunity from treatment discuss the effectiveness and continued use of hygiene measures. The hygiene improvements in Figure 10 can be seen to lower pathogen count and Figures 11 and 12 suggest that more rapid hygienic deterioration leads to a larger number of infected people and a shrinking group of people who can easily catch the disease. All of these findings prove how vital it is to be hygienic to make sure diseases do not spread.

CONCLUSION

This work introduces a detailed model using fractional-order to show cholera transmission which considers immunity relapse, personal hygiene, aspects of the environment and how people behave. Using the modified Caputo derivative and solving the model with LADM, it becomes possible to capture behaviors that can be hard to represent with classical models. Also, the analysis using the Laplace-Adomian Decomposition Method (LADM) confirms the model stays well-defined as the solutions are proper and within expected ranges. Establishing how the basic reproduction number is derived and assessing the stability of any disease in the system provide a strong theoretical background. Simulations based on LADM emphasize that the model can realistically represent cholera behavior in real life, showing its usefulness for public health planning. Evidence shows that cholera lasts longer when people's immunity decreases and hygiene is neglected. Relapse can happen often, especially with poor hygiene, so infection can still be present despite taking action against it. For this reason, strategies to control disease should work on lowering relapse and helping people maintain healthy hygiene to prevent the pathways for infection. Besides cholera, the framework can also be used to analyze other infectious diseases with similar features. With memory effects and adjustable human practices included, this model gives key findings for long-lasting disease prevention strategies and epidemiological forecasts.

REFERENCES

Adedeji, J., & Olayiwola, M. O. (2024). On analysis of a mathematical model of cholera using Caputo fractional order: On analysis of a mathematical model of cholera. Journal of the Nigerian Mathematical Society, 43(3), 287-309.

Adeniyi, E. O. (2024). Transmission dynamics and control of cholera in Africa: A mathematical modelling approach.

Ahmed, I., Akgül, A., Jarad, F., Kumam, P., & Nonlaopon, K. (2023). A Caputo-Fabrizio fractional-order cholera model and its sensitivity analysis. Mathematical Modelling and Numerical Simulation with Applications, 3(2), 170-187.

Ahmad, A., Abbas, F., Farman, M., Hincal, E., Ghaffar, A., Akgül, A., & Hassani, M. K. (2024). Flip bifurcation analysis and mathematical modeling of cholera disease by taking control measures. Scientific Reports, 14(1), 10927.

Alhaji, M. L., Abdullah, F. A., & Mansor, S. N. A. (2024, August). Application of the Laplace-Adomian decomposition method to the dynamics of cholera transmission. In American Institute of Physics Conference Series (Vol. 3189, No. 1, p. 030015).

Ali, A. H., Ahmad, A., Abbas, F., Hincal, E., Ghaffar, A., Batiha, B., & Neamah, H. A. (2025). Modeling the behavior of a generalized cholera epidemic model with asymptomatic measures for early detection. PLoS One, 20(3), e0319684.

Alharbi, M. F. (2025). Neural network procedures for the cholera disease system with public health mediations. Computers in Biology and Medicine, 184, 109471.

Anderson, R. M. & Farrell, S.H. (2018). Helminth lifespan interacts with non-compliance in reducing the effectiveness of anthelmintic treatment. Parasites & vectors, 11(1), 66.

Anteneh, L. M., Lokonon, B. E., & Kakaï, R. G. (2024). Modelling techniques in cholera epidemiology: A systematic and critical review. Mathematical Biosciences, 109210.

Avwerosuo, A. A., & Okedoye, A. M. (2023). Mathematical modelling of the dynamics and control of communicable diseases with emphasis on cholera epidemics. Asian Journal of Applied Science and Technology (AJAST), 7(4), 99-119.

Anwar, N., Fatima, A., Raja, M. A. Z., Ahmad, I., Shoaib, M., & Kiani, A. K. (2025). Novel exploration of machine learning solutions with supervised neural structures for nonlinear cholera epidemic probabilistic model with quarantined impact. The European Physical Journal Plus, 140(1), 64..

Bashiru, K. A., Kolawole, M. K., Ojurongbe, T. A., Adekunle, H. O., Adeboye, N. O., & Afolabi, H. A. (2023). Conceptual analysis of a fractional order epidemic model of measles capturing logistic growth using Laplace Adomian decomposition method. Journal of Applied Computer Science & Mathematics, 17(35).

Cai, G., Li, Y. & Yu, H., (2012). Dynamic analysis and control of a new hyperchaotic finance system. Nonlinear Dynamics, 67(3), 2171-2182.

Dhandapani, P. B., Leiva, V., Martin-Barreiro, C., & Rangasamy, M. (2023). On a novel dynamic of a SIVR model using a Laplace Adomian decomposition based on a vaccination strategy. Fractal and Fractional, 7(5), 407.

Eneh, S., Onukansi, F., Anokwuru, C., Ikhuoria, O., Edeh, G., Obiekwe, S., ... & Okpara, C. (2024). Cholera outbreak trends in Nigeria: Policy recommendations and innovative approaches to prevention and treatment. Frontiers in Public Health, 12, 146436

Farman, M., Sarwar, R., Nisar, K. S., Naik, P. A., Shahzeen, S., & Sambas, A. (2025). Global wave analysis of a fractional-order cholera disease model in society. Network Modeling Analysis in Health Informatics and Bioinformatics, 14(1), 15.

Ghosh, A., Das, P., Chakraborty, T., Das, P., & Ghosh, D. (2025). Developing cholera outbreak forecasting through qualitative dynamics: Insights into Malawi case study. Journal of Theoretical Biology, 605, 112097.

Kolawole, M. K. (2025). Mathematical dynamics of the (SVEITR) model, the impact of treatment and vaccination on cholera spread. Jurnal Diferensial, 7(1), 85-105.

Malik, S. (2024). Numerical performance of the fractional direct spreading cholera disease model: An artificial neural network approach. Fractal & Fractional, 8(7).

Montero, D. A., Vidal, R. M., Velasco, J., George, S., Lucero, Y., Gómez, L. A., ... & O'Ryan, M. (2023). Vibrio cholerae, classification, pathogenesis, immune response, and trends in vaccine development. Frontiers in Medicine, 10, 1155751

Mushanyu, J., Matsebula, L., & Nyabadza, F. (2024). Mathematical modeling of cholera dynamics in the presence of antimicrobial utilization strategy. Scientific Reports, 14(1), 1-22.

Nkwayep, C. H., Kakaï, R. G., & Bowong, S. (2024). Prediction and control of cholera outbreak: Study case of Cameroon. Infectious Disease Modelling, 9(3), 892-925.

Ojo, O. B., & Gbolahan, A. M. (2025). Contextualising cholera in Nigeria: Contemporary epidemiology, determinants and recommendations. ISA Journal of Medical Sciences (ISAJMS), 2(3), 57-68.

Onwunta, I. E., Ozota, G. O., Eze, C. A., Obilom, I. F., Okoli, O. C., Azih, C. N., & Agbo, E. L. (2025). Recurrent cholera outbreaks in Nigeria: A review of the underlying factors and redress. Decoding Infection and Transmission, 3, 100042.

Oweibia, M., Egberipou, T., Wilson, T. R., Timighe, G. C., & Ogbe, P. D. (2025). Factors associated with the propagation of cholera in epidemics across the geopolitical zones of Nigeria: A systematic review. medRxiv, 2025-05.

Ovi, M. A., Afilipoaei, A., & Wang, H. (2025). Estimating hidden cholera burden and intervention effectiveness. Bulletin of Mathematical Biology, 87(6), 1-30.

Rashid, S., Jarad, F., & Alsharidi, A. K. (2022). Numerical investigation of fractional-order cholera epidemic model with transmission dynamics via fractal–fractional operator technique. Chaos, Solitons & Fractals, 162, 112477.

Ratnayake, R. C. (2024). Case-area targeted intervention for the control of cholera epidemics in crises: From spatial mathematical modelling to field evaluation (Doctoral dissertation, London School of Hygiene & Tropical Medicine).

Shah, Z., Ullah, N., Jan, R., Alshehri, M. H., Vrinceanu, N., Antonescu, E., & Farhan, M. (2025). Existence and sensitivity analysis of a Caputo-Fabirizo fractional order vector-borne disease model. European Journal of Pure and Applied Mathematics, 18(2), 5687-5687.

Sit, B., Fakoya, B., & Waldor, M. K. (2022). Emerging concepts in cholera vaccine design. Annual Review of Microbiology, 76(1), 681-702

Trevisin, C., Lemaitre, J. C., Mari, L., Pasetto, D., Gatto, M., & Rinaldo, A. (2022). Epidemicity of cholera spread and the fate of infection control measures. Journal of the Royal Society Interface, 19(188), 20210844.

Wang, J. (2022). Mathematical models for cholera dynamics—A review. Microorganisms, 10(12), 2358.

Yunus, A. O., & Olayiwola, M. O. (2024). The analysis of a co-dynamic ebola and malaria transmission model using the Laplace Adomian decomposition method with Caputo fractional-order. Tanzania Journal of Science, 50(2), 224-243.